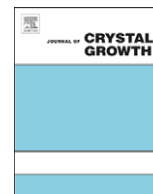




ELSEVIER

Contents lists available at ScienceDirect

Journal of Crystal Growth

journal homepage: www.elsevier.com/locate/jcrysgro

Design and realization of low density InAs quantum dots on AlGaInAs lattice matched to InP(0 0 1)

Roland Enzmann*, Mario Bareiß, Daniela Baierl, Norman Hauke, Gerhard Böhm, Ralf Meyer, Jonathan Finley, Markus-Christian Amann

Walter Schottky Institut¹, Technische Universität München, Am Coulombwall 3, D-85748 Garching, Germany

ARTICLE INFO

Article history:

Received 17 November 2009

Received in revised form

10 May 2010

Accepted 11 May 2010

Communicated by E. Calleja

Available online 16 May 2010

Keywords:

A3. Molecular beam epitaxy

A1. Nanostructures

A1. Quantum dot

B1. InP-substrate

B1. AlGaInAs

B2. 1.55 μm

ABSTRACT

We present detailed growth studies of InAs nanostructures grown on $\text{Al}_x\text{Ga}_y\text{In}_{(1-x-y)}\text{As}$ lattice matched to an InP(0 0 1) substrate using molecular beam epitaxy. Highly elongated quantum dash like structures are typically favoured in this material system, due to very anisotropic migration lengths along the $[1 - 1 0]$ and $[1 1 0]$ directions. In order to increase the short migration length along the $[1 1 0]$ -direction we used ultra low growth rates down to 3×10^{-3} monolayers per second. We show that this offers the possibility to form InAs quantum dots with a low surface density, in contrast to the most commonly formed quantum dash structures. To tailor the emission wavelength of the quantum dots, three methods were studied: (i) the variation of the bandgap of the surrounding material by adjusting the aluminium to gallium ratio, (ii) the variation of the bandgap of the quantum dot material by incorporating antimony and (iii) the variation of the height of the quantum dots by closely stacking two layers of quantum dots upon each other.

© 2010 Elsevier B.V. All rights reserved.

1. Introduction

Self-organized quantum dots can be used for single photon generation and may therefore be key components in quantum information technology [1,2]. In particular for quantum cryptography, single photons have to be transmitted over long distances. For this purpose the photons should be emitted in the optical C-band (1535–1565 nm) to minimize losses in commonly used glass fibres. To obtain single photons using self-assembled quantum dots the light must be generated from a single dot. Thus, to enable a single dot per device a very low quantum dot surface density is needed ($< 5 \mu\text{m}^{-2}$). Low quantum dot densities offer the possibility to investigate single quantum dots via confocal luminescence spectroscopy and to couple single quantum dots to resonator modes e.g. photonic crystal defect modes to obtain a high outcoupling efficiency [3,4]. Self-assembled quantum dots on GaAs substrates have already been extensively studied, but it has proven to be extremely difficult to reach $1.55 \mu\text{m}$, at least for samples with low quantum dot density operated at cryogenic temperatures. In contrast, InP based materials provide emission in the optical C-band. However, the fabrication of InAs quantum dots on InP or on lattice matched AlGaInAs via MBE is a challenge since self-assembled growth often leads to elongated quantum dashes with

a width of 30–40 nm and length up to 500 nm [5–7]. The fabrication of InAs quantum dots on InP(0 0 1) substrates has been demonstrated using metal organic vapour phase epitaxy (MOVPE) applying for instance a “double cap” technique [8] and other technologies [9,10], but these samples exhibit a rather high dot density ($> 100 \mu\text{m}^{-2}$). Accordingly, only very small mesa structures (140 nm diameter) allow the optical isolation of single quantum dots or dashes [11]. Consequently, to realize a single photon emitting device working in the telecommunications band, quantum dots that emit around $1.55 \mu\text{m}$ are required with a low surface density ($< 5 \mu\text{m}^{-2}$). The growth of low quantum dot densities (around $10 \mu\text{m}^{-2}$) in the InAs/InGaAsP/InP-system was recently demonstrated by MOVPE [12].

In this growth study we present a parameter range for the MBE growth of nanostructures in the $\text{Al}_x\text{Ga}_y\text{In}_{(1-x-y)}\text{As}/\text{InP}$ material system wherein the formation of quantum dots with low surface density occurs. Furthermore, we show concepts to controllably adjust the emission wavelength of the dots and to realize a strong confinement for charge carriers to prevent thermal stimulation of excitons out of the quantum dot that reduce the tunnelling rate under electric field.

2. Experimental

All samples were grown in a solid-source molecular beam epitaxy (MBE) system, Varian Mod Gen II on two-inch InP(0 0 1)

¹ URL: <http://www.wsi.tum.de>.

* Corresponding author. Tel.: +49 89 28912759.

E-mail address: Enzmann@wsi.tum.de (R. Enzmann).

substrates. For the growth of the InAs quantum dots we used very low growth rates in contrast to the surrounding $\text{Al}_x\text{Ga}_y\text{In}_{(1-x-y)}\text{As}$. To allow very low growth rates, without growth interruption between the matrix material and the quantum dots, we used a second downward looking indium cell, calibrated using GaAs/GaInAs multi-quantum well structures analyzed by X-ray diffraction. The samples consist of a 400 nm buffer layer $\text{Al}_{0.48}\text{In}_{0.52}\text{As}$ followed by 30 nm $\text{Al}_x\text{Ga}_y\text{In}_{(1-x-y)}\text{As}$ matrix material. Afterwards two regions with quantum dots were deposited: a buried layer for investigation via photoluminescence and a surface layer, separated by a 100 nm $\text{Al}_x\text{Ga}_y\text{In}_{(1-x-y)}\text{As}$ spacer layer, for structural investigations via atomic force microscopy (AFM). To obtain a quantum dot growth independent from the aluminium content in the top most layer at the growth surface, the matrix material was grown as a digital alloy of $\text{Al}_{0.48}\text{In}_{0.52}\text{As}$ and $\text{Ga}_{0.47}\text{In}_{0.53}\text{As}$, which always ends up with a 0.6 nm layer GaInAs. The thicknesses of the $\text{Al}_{0.48}\text{In}_{0.52}\text{As}$ and $\text{Ga}_{0.47}\text{In}_{0.53}\text{As}$ layers were 0.37 and 1 nm, respectively, for the most frequently used $\text{Al}_{0.13}\text{Ga}_{0.35}\text{In}_{0.52}\text{As}$ alloy. This aluminium free surface enables the highest possible mobility of the indium atoms.

2.1. Low growth rates

First of all we analyzed the influences of different indium-fluxes, the growth temperature and the total InAs coverage on the formation of the InAs nanostructures. Fig. 1 shows atomic force microscopy (AFM) graphs taken from the middle of the wafer of samples grown under identical conditions besides the growth rate that was increased from 0.003 monolayers per second (ML/s) to 0.03 ML/s. These four samples were grown with a total InAs coverage of 2.1 monolayers (ML) on $\text{Al}_{0.13}\text{Ga}_{0.35}\text{In}_{0.52}\text{As}$ matrix material. The temperature used for the growth of the samples shown in Figs. 1 (a)–(c) was 495 °C (measured by pyrometer). As the figure shows, a transition from quantum dashes (Fig. 1(a)) with height of 2–3 nm, a width of 30 nm and a length up to 400 nm to chain like arranged quantum dots with a height of 4–5 nm and a diameter of 30 nm (Fig. 1(b)) can be observed while lowering the growth rate from 0.03 to 0.006 ML/s. A further reduction of the growth rate to 0.003 ML/s leads to the formation of single quantum dots with a height of 3–4 nm and a diameter of 25–30 nm (Fig. 1(c)). Very low growth rates provide long migration times for the arriving indium atoms and therefore make high migration lengths possible. The migration length can also be enhanced by raising the growth temperature. The sample in Fig. 1(d) was grown with 0.006 ML/s, which is the same rate used for the sample shown in Fig. 1(b) but at a higher temperature (505 °C pyrometer). The quantum dots grown under these conditions have a diameter of 30 nm and a height of 3–5 nm. They are not as homogeneous as the quantum dots grown with 0.003 ML/s at 495 °C but therefore also higher quantum dots (around 5 nm) appear. Aiming for a strong carrier confinement we used these conditions for further studies, to fabricate high quantum dots with lower quantisation energy. Using the parameters corresponding to Fig. 1(c) and (d), we realized low density quantum dots ($\sim 4 \mu\text{m}^{-2}$) within an InAs coverage of 2.1–2.6 monolayers. Corresponding to growth parameters that allow long migration lengths or migration times, respectively, for the arriving indium atoms, we observe a transition from quantum dash like structures via chain like structures to single quantum dots in a low surface density. It is important to point out that we observed formation of quantum dots only when using very low growth rates from 0.003 to 0.006 ML/s as shown in Fig. 1(b) and (c). Due to an exponential dependence of the indium desorption rate on the growth temperature, a high mobility of the indium atoms operating at higher temperatures is not practical.

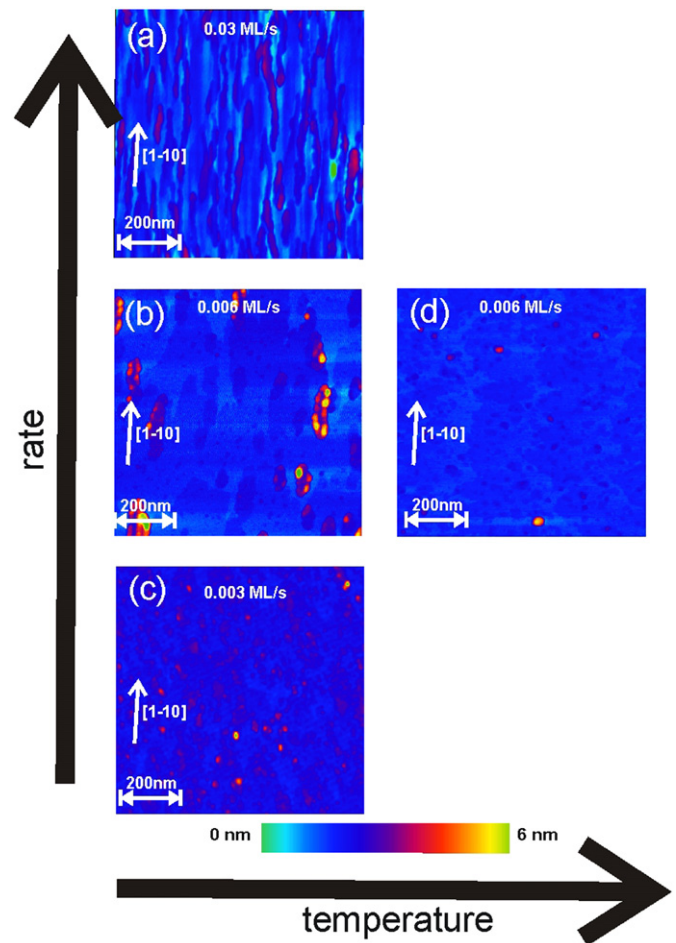


Fig. 1. AFM-micrographs ($1 \mu\text{m}^2$) show a transition from dash- to dot-like structures lowering the growth rate from (a) 0.03 ML/s and 495 °C, (b) 0.006 ML/s and 495 °C to (c) 0.003 ML/s and 495 °C. Sample (d) shows similar density and geometry like sample (c), it is grown with 0.006 ML/s and 505 °C pyrometer temperature. All samples have an InAs coverage of 2.1 ML.

In the following, we discuss the optical properties of the buried layer of quantum dots grown under similar conditions to the samples shown in Fig. 1. Photoluminescence measurements were taken from single quantum dots using a confocal micro-photoluminescence setup. A helium–neon-laser operating at 623.8 nm was used for optical excitation. This laser was focused on the sample using an M-Plan NIR objective with a numerical aperture of 0.55. All measurements were performed at 10 K with the samples mounted in a helium flow cryostat. The photoluminescence light was detected using a Triax-550 spectrometer combined with an InGaAs-photodiode array. Due to the low quantum dot density no patterning of the sample is required to perform optical experiments on single quantum dots. Typical micro-photoluminescence spectra are shown in Fig. 2. The figure shows several samples with low density quantum dots. To achieve emission in the optical C-band, the wavelength tuning was performed by adjusting the bandgap of the surrounding $\text{Al}_x\text{Ga}_y\text{In}_{(1-x-y)}\text{As}$ matrix material using different contents of aluminium and gallium. Three samples were fabricated with aluminium contents of 48%, 13% and 4%. Lowering the bandgap of the matrix material leads to lower quantisation energy in the quantum dot and therefore to a longer wavelength of the emission.

Due to the digital alloy growth mode, the total aluminium in the barrier material has only a minor influence on the formation of the nanostructures. As can be seen in Fig. 2(a) an emission

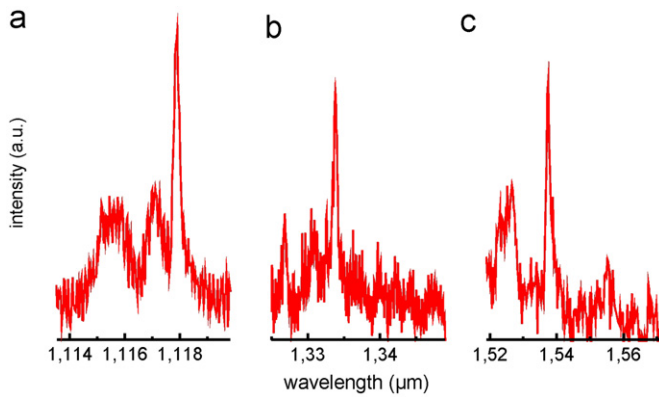


Fig. 2. Emission from single quantum dots with different aluminium contents in the matrix material: (a) 48%, (b) 13% and (c) 4%.

around 1.1 μm corresponds to an $\text{Al}_{0.48}\text{In}_{0.52}\text{As}$ alloy. Lowering the aluminium content to 13% an emission around 1.3 μm was realized (optical O-band (Fig. 2(b))), a further reduction to 4% aluminium leads to an emission from the quantum dots within the optical C-band around 1.55 μm as shown in Fig. 2(c). All samples exhibit an inhomogeneous broadening around 80 nm.

The corresponding matrix material of the quantum dots shown in Fig. 2(c) emits around 1.55 μm , so the binding energy of the confined exciton is very low. The binding energy of the electron was estimated by calculation of the bandstructure using the software nextnano³ to less than 10 meV. In order to tune the quantum dot emission by temperature or by an electric field using the quantum confined Stark effect [13], a higher carrier confinement is beneficial. This leads to an improved thermal stability of the luminescence intensity, a drastically reduced carrier tunnelling escape rate and, thus, a larger tuning range via an applied electric field before luminescence quenches due to e–h tunnelling [14,15]. Thus the transition energy of the exciton must be held constant while the bandgap of the barrier material is increased. There are two possibilities to realize this: to decrease the bandgap of the quantum dot material or to increase the height of the quantum dots. Both effects decrease the transition energy and, therefore, counteract the blue shift caused by introducing a higher bandgap barrier matrix material.

2.2. Using antimony

To decrease the bandgap of the quantum dot material, we investigated the possibility to incorporate antimony into the InAs quantum dots. Based on the $\text{Al}_{0.13}\text{Ga}_{0.35}\text{In}_{0.52}\text{As}$ matrix material an incorporation of 10% antimony into the InAs quantum dots should lead to a red shift of about 100 nm. Fig. 3 shows AFM images of a series of samples grown on an $\text{Al}_{0.13}\text{Ga}_{0.35}\text{In}_{0.52}\text{As}$ matrix material with a total InAs coverage of 2.1 ML. For all samples we used an indium flux of 0.006 ML/s and a growth temperature of 505 $^{\circ}\text{C}$ (pyrometer). The antimony incorporation was calibrated using InAsSb/GaInAs (0.6 nm/25 nm) multiple quantum well structures analyzed by X-ray diffraction. The quantum dots in Fig. 3(a) were fabricated by simultaneously offering arsenic and antimony during the nanostructure growth. As known from the growth of nanostructures on GaAs substrates, antimony acts as a surfactant and generates many nucleation sites for quantum dots [16]. Therefore, the quantum dot density increased up to ~ 200 dots per μm^2 . In order to achieve low densities, it is necessary to inhibit the surfactant effect of antimony. The quantum dots shown in Figs. 3(b) and (c) were grown in two steps: first a 1.8 ML thick InAs layer was deposited, close to the critical thickness for quantum dot growth. The last

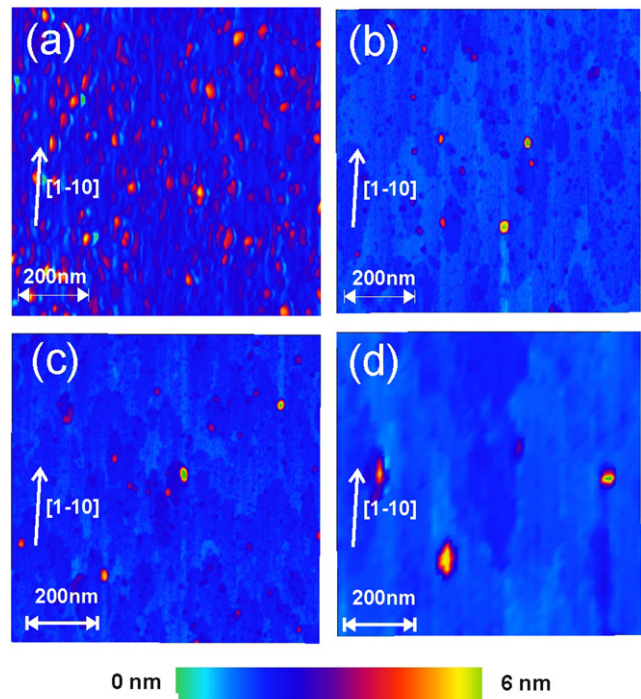


Fig. 3. AFM-micrograph ($1 \mu\text{m}^2$) of InAs(Sb) quantum dots on $\text{Al}_{0.13}\text{Ga}_{0.35}\text{In}_{0.52}\text{As}$: (a) 2.1 ML $\text{InAs}_{0.8}\text{Sb}_{0.2}$ quantum dots, (b) 1.8 ML InAs and 0.3 ML $\text{InAs}_{0.9}\text{Sb}_{0.1}$, (c) 1.8 ML InAs and 0.3 ML $\text{InAs}_{0.8}\text{Sb}_{0.2}$ and (d) 2.1 ML InAs with 20 s antimony irradiation.

0.3 ML of the quantum dot materials were grown as alloy of $\text{InAs}_x\text{Sb}_{1-x}$ using $x=10\%$ and 20% antimony, respectively. The sample shown in Fig. 3(c) was exposed to an antimony flux (beam equivalent pressure 1.77×10^{-6} Torr) for 20 sec after the InAs quantum dots growth. As both figures show, there is no significant change in the quantum dot morphology as compared to the sample shown in Fig. 1(d) grown without antimony. Microphotoluminescence measurements of single quantum dots grown in the similar growth mode to those shown in (Figs. 3(b)–(d)) were also performed and showed no significant red shift of the emission compared to a reference sample grown without antimony. Furthermore, a rapid decrease in optical quality of the quantum dots for higher antimony content than 10% was observed. However, a red shift from 1260 to 1310 nm of the emission of the matrix material and wetting layer is a good evidence for strong intermixing with the overgrown material. The reason for this intermixing may lie in phase separation phenomena of InAsSb/GaInAs to InAs and GaSb rich areas at the interfaces occurring during overgrowth in this material system [17]. In conclusion it can be asserted, that no incorporation of antimony into the quantum dots could be observed.

2.3. Stacked layers of quantum dots

The second way to achieve higher carrier confinement together with an emission wavelength around 1.5 μm is to grow larger quantum dots. In particular taller dots produce a strong red shift of the emission energy. One way to realize taller quantum dots is to vertically stack them on each other. This can be realized by a two step growth mode. Two layers of quantum dots, separated by a thin spacer layer are grown upon each other, this can cause also a vertical alignment and is a well know technique for InAs quantum dots grown on GaAs substrates [18–20]. Furthermore, for the InAs/GaAs material system it is also reported that vertical aligned quantum dots merge to a single larger dot, when very low

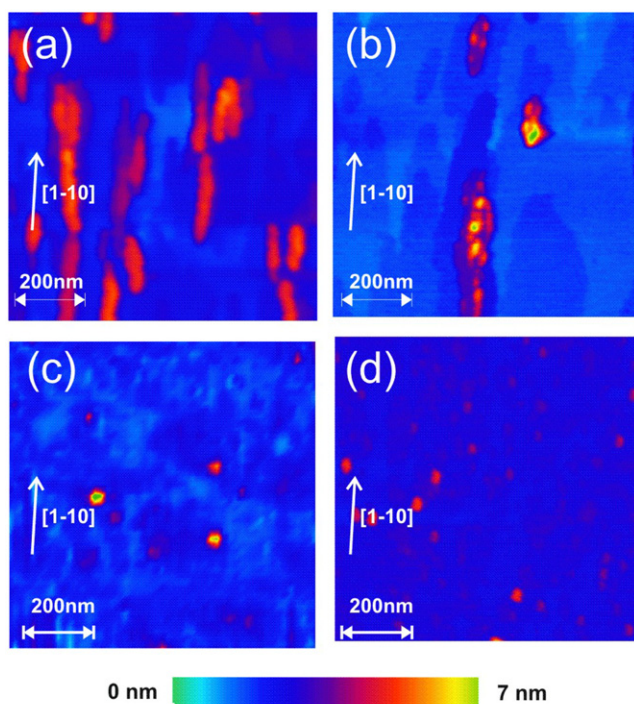


Fig. 4. AFM-micrograph ($1 \mu\text{m}^2$) of an uncapped stacked dot sample with varying InAs coverages of the top layer: (a) 2.1 ML, (b) 1.8 ML, (c) 1.5 ML and (d) 1.3 ML.

growth rates are used [21]. Hence, several samples with two layers of quantum dots were fabricated, using a spacer thickness in the range of the quantum dot height from 3.1 nm. The InAs coverage of the top layer was varied from 1.3 to 2.1 ML, with coverages of 1.3, 1.5, 1.8, and 2.1 ML. A sample grown under the same conditions than the one shown in Fig. 1(d) serves as seed layer and both layers were grown with a growth rate of 0.006 ML/s using a growth temperature of 505 °C (pyrometer). All samples were embedded in $\text{Al}_{0.20}\text{Ga}_{0.27}\text{In}_{0.53}\text{As}$ matrix material. Characterization was done by AFM on uncapped samples and micro photoluminescence on capped samples. Fig. 4 shows the corresponding AFM images of the uncapped stacked dot structures. As can be seen from the figure, for the sample with 2.1 monolayers coverage on the top layer predominantly dash like structures with a height from 3 to 4 nm occur (Fig. 4(a)). Lowering the InAs coverage to 1.8 ML a transition from dash- to dot-like nanostructures take place as shown in Fig. 4(b). Using a coverage of 1.5 ML resulted in quantum dots with a low surface density and a height around 3–5 nm (Fig. 4(c)). For the sample with coverage of 1.3 ML only quantum dots with a height less than 3 nm were formed (Fig. 4(d)). Fig. 5 shows a micro-photoluminescence measurement of a sample with 3.1 nm spacer layer and an InAs coverage of 1.5 ML of the upper layer. Photoluminescence of the matrix material around 1.2 μm can be seen in the figure. Emission from uncapped quantum dots for the $\text{Al}_{0.20}\text{Ga}_{0.27}\text{In}_{0.53}\text{As}$ matrix material is expected to be around 1.27 μm . In contrast to this, the measurements of the double layer show a long wavelength luminescence peaks at 1.44 and 1.47 μm , which is an evidence that the dots stacking approach at low density conditions allows to get a longer wavelength emission. Even at very low excitation powers around 5 nW photoluminescence of these quantum dots could be measured. This argues for a high optical quality together with higher confinement of the charge carriers and therefore better characteristics at higher temperatures and under electrical fields.

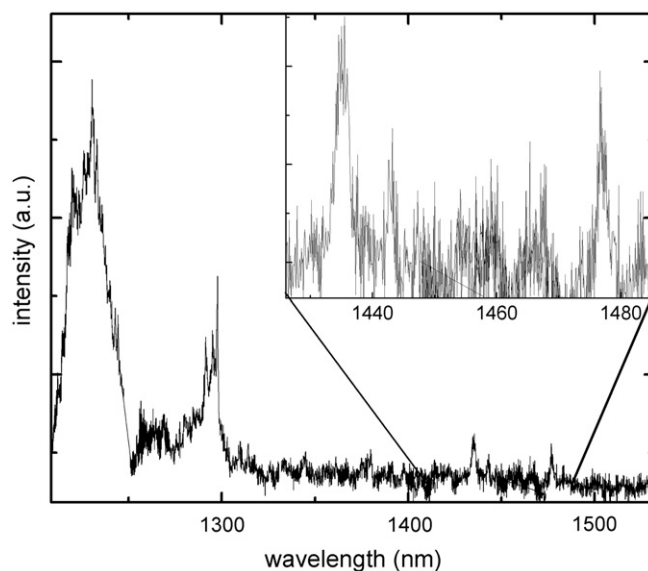


Fig. 5. Micro-photoluminescence measurement of a double layer of quantum dots with a spacer thickness of 3 nm and a coverage of the second layer of 1.5 ML. The inset shows an enlargement of the marked part of the spectrum.

3. Conclusion

In summary, we presented an MBE growth process for InAs quantum dots on AlGaInAs in a low surface density using very low growth rates. Depending on the matrix material emission between 1.1 and 1.55 μm could be realized. Two concepts to increase the carrier confinement are presented. Whereas the incorporation of antimony into the quantum dots did not succeed, a successful fabrication of vertical aligned quantum dots was performed. There is still room for optimization of this growth mode, but nevertheless these quantum dots can be promising sources for single photon generation at both telecommunication wavelengths regimes.

Acknowledgement

This project was supported by the German excellence cluster “Nanosystems Initiative Munich (NIM)”.

References

- [1] P. Michler, A. Kiraz, C. Becher, W.V. Schoenfeld, P.M. Petroff, L. Zhang, E. Hu, A. Imamoglu, A quantum dot single-photon turnstile device, *Science* 290 (2000) 5500.
- [2] N. Gisin, G. Ribordy, W. Tittel, H. Zbinden, Quantum cryptography, *Rev. Mod. Phys.* 74 (2002) 145.
- [3] M. Kaniber, A. Kress, A. Laucht, M. Bichler, R. Meyer, M.-C. Amann, J.J. Finley, Efficient spatial redistribution of quantum dot spontaneous emission from two-dimensional photonic crystals, *Appl. Phys. Lett.* 91 (2007) 061106.
- [4] A. Kress, F. Hofbauer, N. Reinelt, M. Kaniber, H.J. Krenner, R. Meyer, G. Böhm, J.J. Finley, Manipulation of the spontaneous emission dynamics of quantum dots in two-dimensional photonic crystals, *Phys. Rev. B* 71 (2005) 241304(R).
- [5] M.U. Gonzales, L. Gonzales, J.M. Garcia, Y. Gonzales, J.P. Silveira, F. Briones, Stress evolution aspects during InAs/InP (001) quantum wires self-assembly, *Microelectron. J.* 35 (2004) 13.
- [6] A. Sauerwald, T. Kuemmel, G. Bacher, A. Somers, R. Schwertberger, J.P. Reithmaier, A. Forchel, Size control of InAs quantum dashes, *Appl. Phys. Lett.* 86 (2005) 253112.
- [7] G. Balakrishnan, S. Huang, L.R. Dawson, D.L. Huffaker, Analysis of atomic structure in InAs quantum dashes grown on AlGaAsSb metamorphic buffers, *J. Vac. Sci. Technol.* 22 (2004) 1529.
- [8] K. Takemoto, Y. Sakuma, S. Hirose, T. Ususki, N. Yokoyama, Observation of exciton transition in 1.3–1.55 μm band from single InAs/InP quantum dots in mesa structure, *Jpn. J. Appl. Phys.* 43 (2004) L349–L351.

- [9] G. Saint-Girons, A. Michon, I. Sagnes, G. Beaudoin, G. Patriarche, Thermodynamic description of the competition between quantum dots and quantum dashes during metalorganic vapor phase epitaxy in the InAs/InP(001) system: experiment and theory, *Phys. Rev. B* 74 (2006) 245305.
- [10] X.B. Zhang, J.H. Ryou, R.D. Dupuis, Growth of InAlAs self-assembled quantum dots on InAlGaAs/InP for 1.55 μm laser applications by metalorganic chemical vapor deposition, *Appl. Phys. Lett.* 89 (2006) 191104.
- [11] G. Sek, P. Podemski, A. Musial, J. Misiewicz, S. Hein, S. Hofling, A. Forchel, Exciton and biexciton emission from a single InAs/InP quantum dash, *J. Appl. Phys.* 105 (2009) 086104.
- [12] P.J. van Veldhoven, N. Chauvin, A. Fiore, R. Nötzel, Low density 1.55 μm InAs/InGaAsP/InP (1 0 0) quantum dots enabled by an ultrathin GaAs interlayer, *Appl. Phys. Lett.* 95 (2009) 113110.
- [13] D.A.B. Miller, D.S. Chemla, T.C. Damen, A.C. Gossard, W. Wiegmann, T.H. Wood, C.A. Burrus, Band-edge electroabsorption in quantum well structures: the quantum-confined Stark effect, *Phys. Rev. Lett.* 53 (1984) 2173.
- [14] W. Yang, R.R. Lowe-Webb, H. Lee, P.C. Sercel, Effect of carrier emission and retrapping on luminescence time decays in InAs/GaAs quantum dots, *Phys. Rev. B* 56 (1997) 13314.
- [15] P.W. Fry, J.J. Finley, L.R. Wilson, A. Lemaitre, D.J. Mowbray, M.S. Skolnick, M. Hopkinson, G. Hill, J.C. Clark, Electric-field-dependent carrier capture and escape in self-assembled InAs/GaAs quantum dots, *Appl. Phys. Lett.* 77 (2000) 4344.
- [16] M. Kudo, T. Nakaoka, S. Iwamoto, Y. Arakawa, InAsSb quantum dots grown on GaAs substrates by molecular beam epitaxy, *Jpn. J. Appl. Phys.* 44 (2005) L45–L47.
- [17] R.M. Biefeld, K.C. Baucom, S.R. Kurtz, D.M. Follstaedt, Proceedings of (MRS), Boston, MA (United States), 29 November–3 December 1993.
- [18] G.S. Solomon, J.A. Trezza, A.F. Marshall, J.S. Harris, Structural and photoluminescence properties of growth-induced InAs island columns in GaAs, *J. Vac. Sci. Technol. B* 14 (1996) 2208.
- [19] B. Lita, R.S. Goldman, J.D. Phillips, P.K. Bhattacharya, Nanometer-scale studies of vertical organization and evolution of stacked self-assembled InAs/GaAs quantum dots, *Appl. Phys. Lett.* 74 (1999) 2824.
- [20] G.S. Solomon, J.A. Trezza, A.F. Marshall, J.S. Harris, Vertically aligned and electronically coupled growth induced InAs islands in GaAs, *Phys. Rev. Lett.* 76 (1996) 952.
- [21] H. Heidemeyer, S. Kiravittaya, C. Muller, N.Y. Jin-Phillipp, O.G. Schmidt, Closely stacked InAs/GaAs quantum dots grown at low growth rate, *Appl. Phys. Lett.* 80 (2002) 1544.